Progress In Electromagnetics Research C, Vol. 77, 69–80, 2017

Dielectric Slabs Covered Broadband Vivaldi Antenna for Gain Enhancement

Xiang Xiang Li[1], Dong Wei Pang[1], Hai Lin Wang[2], Yan Mei Zhang[3], and Guo Qiang Lv[1, *]

Abstract—To enhance the gain of conventional Vivaldi antenna (CVA), a novel dielectric sheets-covered Vivaldi antenna (DSCVA) is proposed. The dielectric sheets suck energy from the tapered slot region and flare termination region of the CVA, and thus act as surface wave antennas to improve end-fire performances. The CVA, DSCVA as well as the DSCVA with elongated tapered profile (SP-DSCVA) are designed, fabricated and measured. The simulation results are in good agreement with the experimental data. Measurement results show that the gain increase of the DSCVA is up to 5.1 dBi in the range of 3.5–16.5 GHz without increasing antenna length compared to the CVA. More gain enhancement is achieved for the SP-DSCVA. In addition, the half power beamwidths of the CVA as well as the sidelobe levels are improved in both E- and H-planes.

1. INTRODUCTION

Vivaldi antenna, also called exponential tapered slot antenna (TSA), has various promising features including broadband, end-fire radiation, low impulse distortion, geometric simplicity, and ease of fabrication. Since it was proposed by Gibson, it has been extensively used in ultra-wideband applications, microwave imaging system, radio telescope, wireless communication, and radar [1–4]. However, some challenging issues on the conventional Vivaldi antenna (CVA) including instable radiation pattern, main beam tilt and split, low gain at high frequencies draw many researchers' attention.

Some measures have been proposed to solve the issues. The coplanar lens produced by substrate end shaping technique, director made of a profiled dielectric piece with higher permittivity, hemisphere lens placed in front of the antenna, and metal director formed by parasitic patch have been proposed to produce directed radiation pattern and enhance antenna gain [5–11]. The corrugation edge technique is proposed to improve radiation features of lower frequencies [12–14]. Double-slot (DS) structure of the Vivaldi antenna in [15, 16] can generate uniform aperture field distribution, which leads to achieving higher gain than the CVA with same size. Artificial materials including anisotropic zero refractive index metamaterial (AZIM), negative index metamaterial (NIM), and high refractive index metamaterial (HIM) were employed to enhance the gain of TSA [17–21]. Additionally, combination of different methods has been utilized by many researchers [2, 8, 16, 21, 22]. Although the above-mentioned methods can improve antenna performance effectively, some deficiencies such as long antenna length, limited gain increase, complicated structure, narrow frequency band, and high cost restrict their applications.

In this paper, a novel simple dielectric sheets-covered Vivaldi antenna (DSCVA) is proposed with improved performances. The dielectric sheets couple space waves from the CVA. Then these space

Received 3 July 2017, Accepted 15 August 2017, Scheduled 23 August 2017

* Corresponding author: Guo Qiang Lv (guoqianglv@hfut.edu.cn or microwaveb@126.com).

[1] Key Laboratory of Special Display Technology of the Ministry of Education, National Engineering Laboratory of Special Display Technology, National Key Laboratory of Advanced Display Technology, Academy of Photoelectric Technology, Hefei University of Technology, Hefei 230009, China. [2] State Key Laboratory of Millimeter Waves, School of Information Science and Engineering, Southeast University, Nanjing 210096, China. [3] Radar Research Laboratory, Beijing Institute of Technology, Beijing 100081, China.

waves are transformed into surface waves and radiate in the end-fire direction. This method can achieve substantial gain increase without increasing the overall antenna length. Besides, to further achieve higher gain, the DSCVA with elongated and tapered profile aiming at increasing the radiation efficiency of surface wave is designed. The prototypes of the CVA and proposed antennas are all fabricated and measured. Measurement results show that the gain of the DSCVA in the band of 3.5–16.5 GHz is 5.3–13.1 dBi, while it is 5.72–15.3 dBi for the SP-DSCVA. The gain enhancement up to 5.3 and 7.6 dBi is achieved compared to the CVA, respectively. The proposed structure can also reduce the side-lobe level and half-power beamwidth.

2. ANTENNA DESIGN AND DISCUSSION

The geometry of the proposed antenna is demonstrated in Fig. 1(a). It consists of two major parts: the original CVA and two same dielectric sheets. The design of the original CVA is based on the previous structure in [22] that is designed for our microwave imaging device. To achieve higher gain in wider frequency band, the dielectric sheet spaced by an air layer is introduced to in this paper. The detailed design process is described as follows.

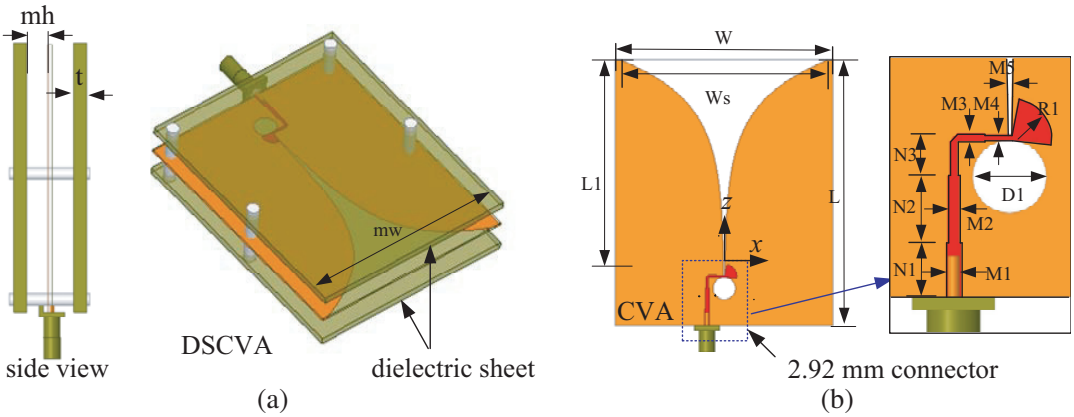

Figure 1. Structures of (a) the proposed DSCVA and (b) the original CVA.

2.1. Design of the CVA

The configuration of the original CVA is illustrated in Fig. 1(b). The values of antenna structural parameters come from [22] and are listed in Table 1. The prototype is printed on a Rogers RO4003C substrate with dielectric constant of 3.38 and loss tangent of 0.0027. Thickness of the substrate is 0.508 mm. The CVA includes a two-step quarter wavelength transition between microstrip line and slotline for impedance matching and a main exponential slot radiator. HFSS simulation is used to evaluate the performances of the CVA considering the effect of coaxial connector. The simulated reflection coefficient S_{11} of the CVA in Fig. 2(a) shows that the impedance bandwidth of the antenna with $S_{11} < -10$ dB is in the range of 3.5–16.5 GHz. The simulated gain variation of the CVA is illustrated in Fig. 2(b). It can be observed that the antenna gain starts to descend at the frequency of 11.5 GHz.

Table 1. Design parameters of the antennas and their dimensions (unit: mm).

parameters	L	W	$L1$	mw	t	mh	$D1$	$R1$
value	64	52	50	25	1.524	5	5.4	2.9
parameters	$N1$	$N2$	$N3$	$M1$	$M2$	$M3$	$M4$	$M5$
value	4.4	5	2.5	1.1	0.87	0.54	0.4	0.3

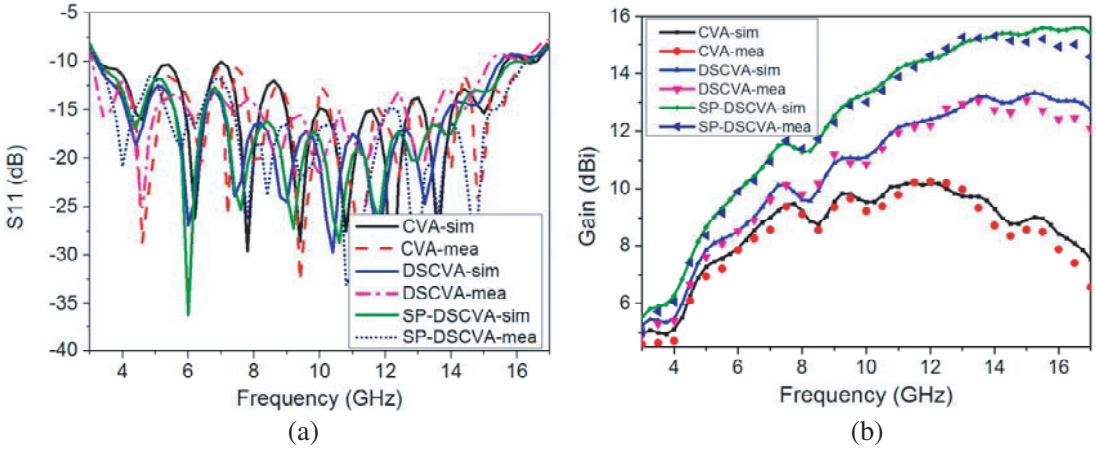

Figure 2. Simulated and measured results of (a) reflection coefficient S_{11} and (b) gain.

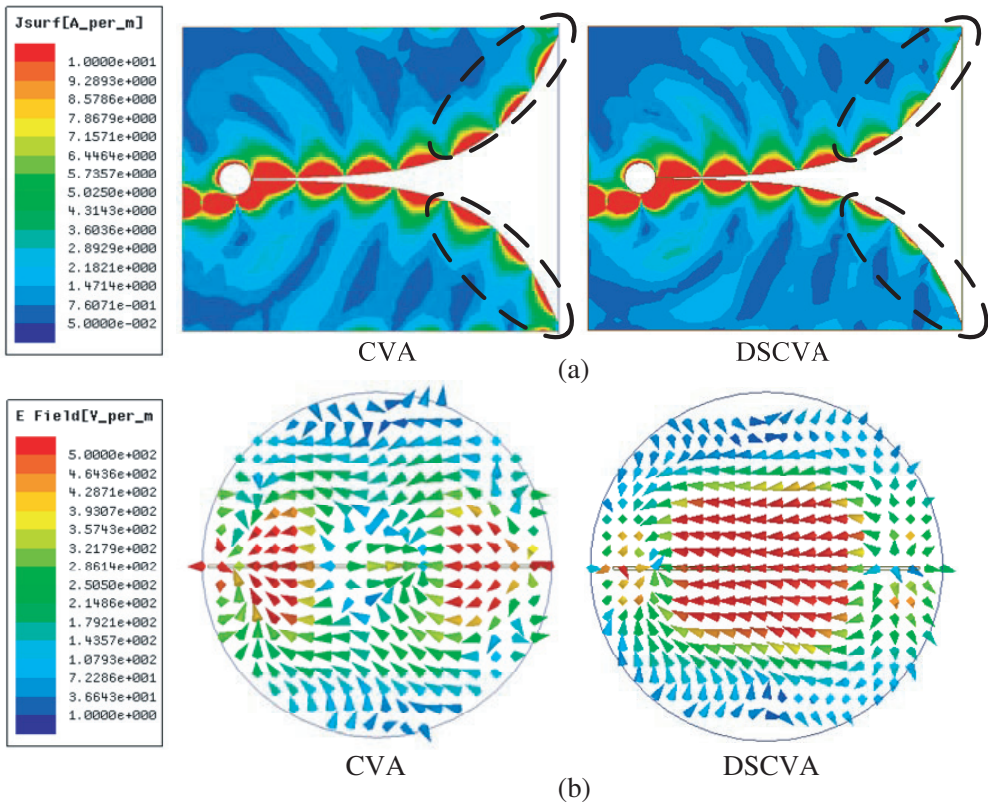

Figure 3. Distribution of (a) surface current and (b) aperture vector E-field at 15 GHz.

The decrease of the antenna gain results from the travelling currents at the flare termination shown in Fig. 3(a) as well as the spherical wave mode leading to the phase errors at the radiation aperture.

2.2. Proposed DSCVA and Discussion

2.2.1. Radiation Mechanism of the DSCVA

The CVA belongs to the class of traveling wave antennas of the 'surface-wave' type [23]. As illustrated in Fig. 4(a), part of the EM waves propagate along the tapered slot in the form of surface waves with

a phase velocity lower than the speed of light and then radiate in the end-fire direction; the other part produced by higher order Hankel Function modes radiate into the free air from the antenna board in the form of space waves [1]. To guide the EM waves towards the aperture center and realize high gain, the dielectric sheet which can support surface wave propagating along the air-dielectric interface is introduced in close proximity to the antenna board. Fig. 1(a) depicts configuration of the proposed DSCVA.

As plotted in Fig. 4(b), the dielectric slabs couple with the CVA, and then transform the space waves emanating from the CVA to the guide waves, resulting in the dielectric sheets to be the simplest dielectric sheet radiators. The intensity of travelling current along the flare section gradually weakens as the EM energy is coupled into the dielectric slabs. Fig. 3(a) illustrates the surface current distributions of the CVA and DSCVA at 15 GHz, respectively. It is evident that the surface current density in the flare termination of the DSCVA is weaker than that of the CVA. To further explain the impact of the EM coupling, the E-field distributions on the antenna surface ($y = 0$, E-plane), dielectric sheet surface ($y = 5.75$ mm), and YZ-plane (H-plane) are shown in Fig. 5, respectively. From Figs. 5(a)–5(b), it is clear that intensity of E-field in the tapered slot is reduced especially at the flare termination, while being enhanced in the dielectric sheet due to the coupling. The phenomenon that the transmitted E-field is gradually coupled to the dielectric sheets can be more remarkably seen from the H-plane E-field distribution in Fig. 5(c). Furthermore, by converting the space waves into surface waves possessing the same phase velocity as those on the antenna board, phase distribution of E-field at the antenna aperture

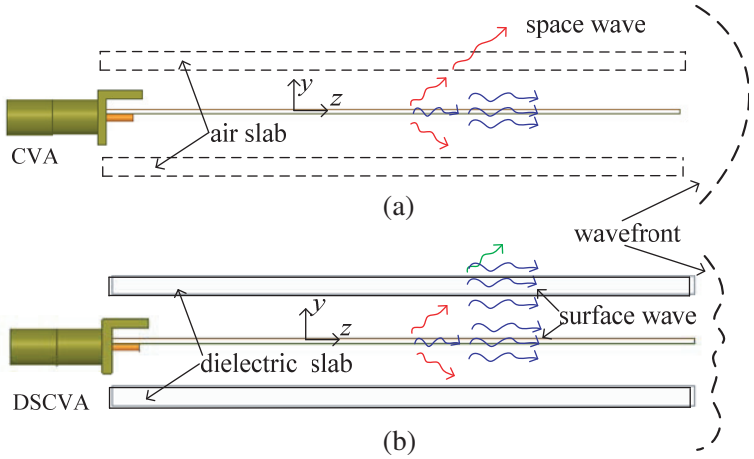

Figure 4. Schematic diagram of EM waves emit from the antenna board. (a) CVA, (b) DSCVA.

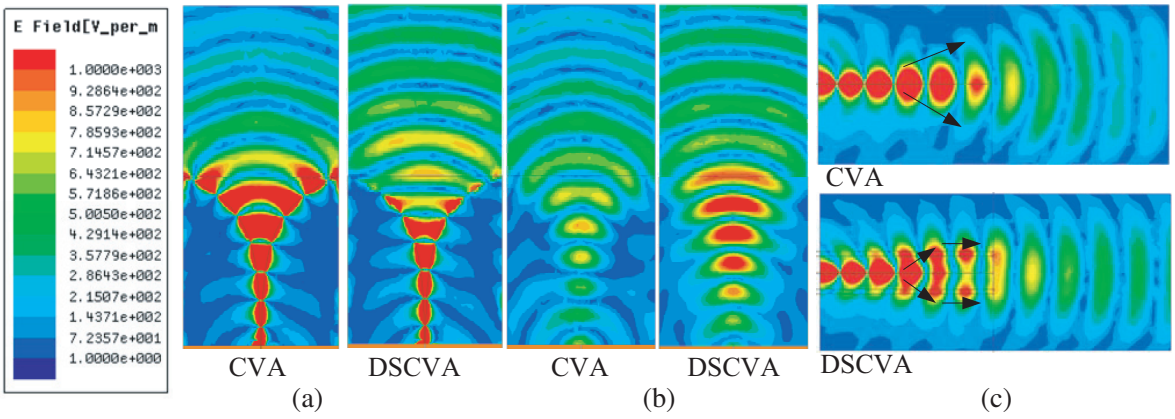

Figure 5. Distribution of E-field on the (a) E-plane (XZ-plane), (b) dielectric sheet surface ($y = 5.75$ mm), and (c) H-plane (YZ-plane).

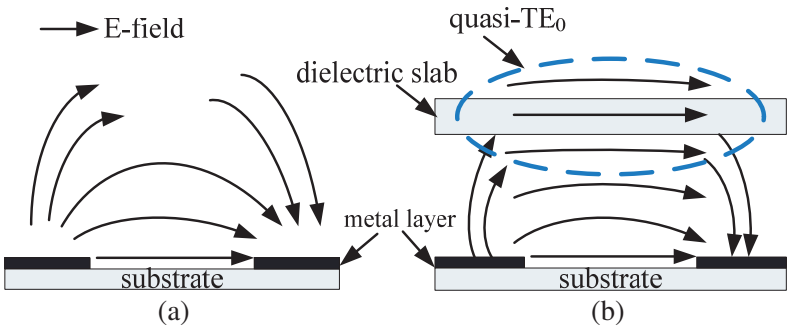

Figure 6. Illustration of mode conversion.

becomes more uniform which contributes to producing directive beam. This can also be explained from the mode conversion, as shown in Fig. 6. With the dielectrics, the radiation modes in the free air are transformed to the quasi surface wave dominant TE mode of the dielectric sheet. As shown in Fig. 3(b), vector E-field distribution of the circular aperture with radius of 27 mm on the plane of $z = 50$ mm indicates that the DSCVA really shows smoother wavefront in the main radiation area than the CVA.

2.2.2. Design Procedure

According to the operating principle of the Vivaldi antenna, the primary radiation occurs in the exponentially tapered slot. The width of the dielectric sheet is therefore designated as the opening width of the tapered slot of the CVA to ensure that the energy can be concentrated in the slot region. It is important to mention that the performances of the proposed antenna are mainly determined by the separation mh between dielectric sheet and antenna substrate, as well as the parameters of dielectric sheet including permittivity and thickness t.

The former affects the effective radiation aperture. Fig. 7 plots the antenna aperture vector E-field distributions at 15 GHz when the separation increases from 3 mm to 7 mm, as well as the gain curve of the proposed antenna over entire frequency band. It can be found that the size of the effective aperture varies with the separation, and by selecting a proper separation, the antenna gain increases due to the energy focusing in the middle region. It is determined that the optimal separation mh is approximately quarter wavelength of the high end frequency so that the electrical fields at high frequencies gather inside and around the cavity formed by the dielectric sheets. For the operational range of 3–17 GHz, we select the separation mh as quarter wavelength of frequency of 15 GHz (= 5 mm).

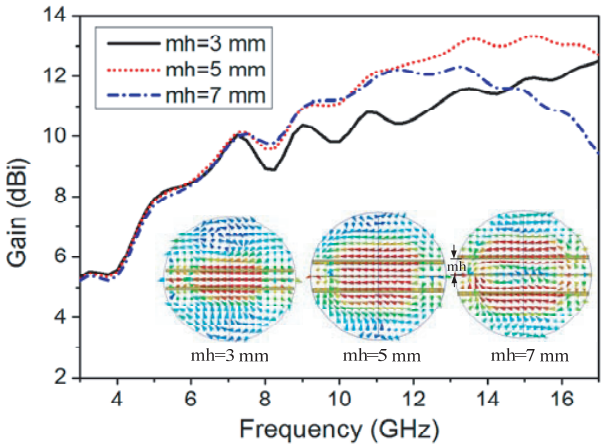

Figure 7. Aperture vector E-field distribution at 15 GHz with different separations. Color bar of amplitude range is shown in Fig. 3(b).

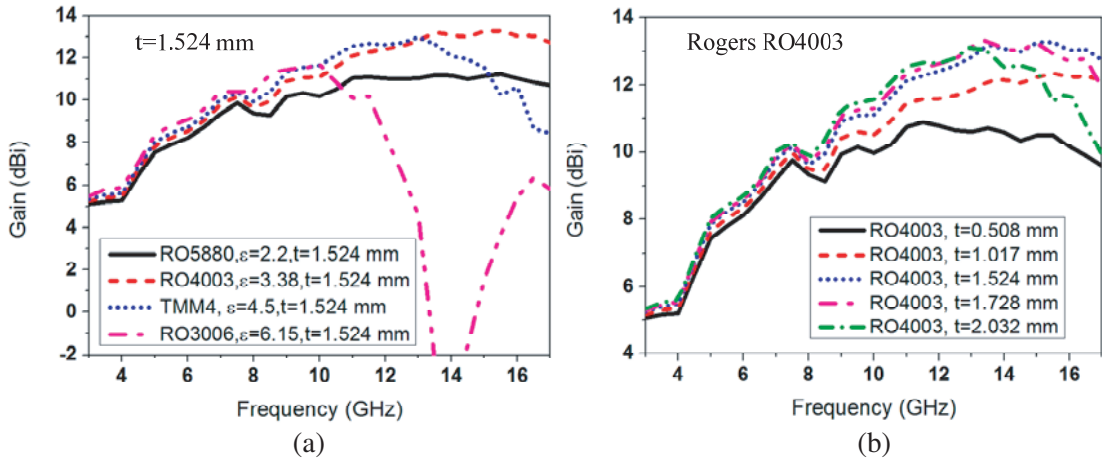

Figure 8. Comparison of gain curves for the DSCVA. (a) The thickness of dielectric sheet is 1.524 mm with different permittivity and (b) the dielectric sheet is adopted as RO4003 with different thicknesses.

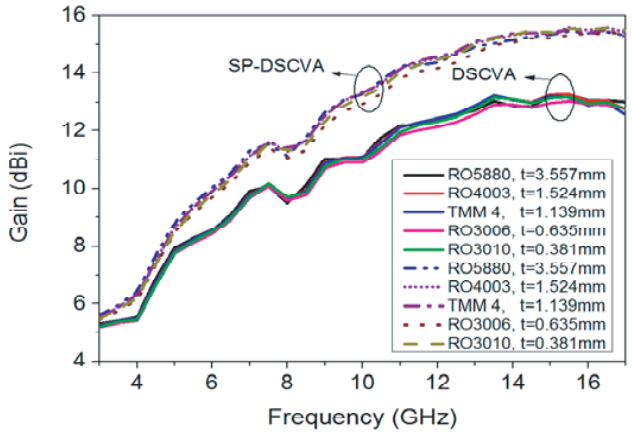

Figure 9. The optimum gain variations for DSCVA and SP-DSCVA with different dielectric sheet and appropriate thickness.

The latter affects the coupling efficiency between the CVA and dielectric sheets. Figs. 8(a) and (b) present gain of the CVA covering different permittivity dielectric materials with same thickness of 1.524 mm and same dielectric sheets made of Rogers RO4003C with different thicknesses, respectively. The thorough parametric study results show that high permittivity and thick dielectric can achieve better antenna performance in a narrow bandwidth. To enhance gain of the CVA in a broad bandwidth, a compromise between permittivity and thickness should be made. Fig. 9 plots optimum gain variations of the DSCVA for several common materials with appropriate thickness. It is obvious that all the cases provide good performances. The gain curves of the DSCVA with different materials have similar trends.

2.3. Proposed SP-DSCVA

The typical way for increasing the efficiency of the surface wave radiation is to elongate and taper the profile of the dielectric sheets. To further achieve higher gain, the elongated DSCVA with shaped profile is designed as shown in Fig. 10. The effect of profile shape (elliptical-shaped, rectangular-shaped, trapezoid-shaped, and triangular-shaped) on antenna boresight gain is investigated. The results in Fig. 11(a) show that the trapezoid-shaped profile is the best candidate for realizing high gain over wideband, and then the elliptical-shaped profile. This is because the trapezoid-shaped profile can

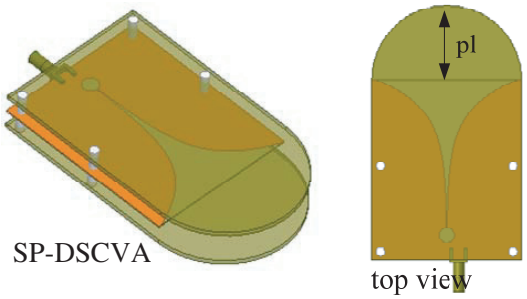

Figure 10. Configuration of the proposed SP-DSCVA.

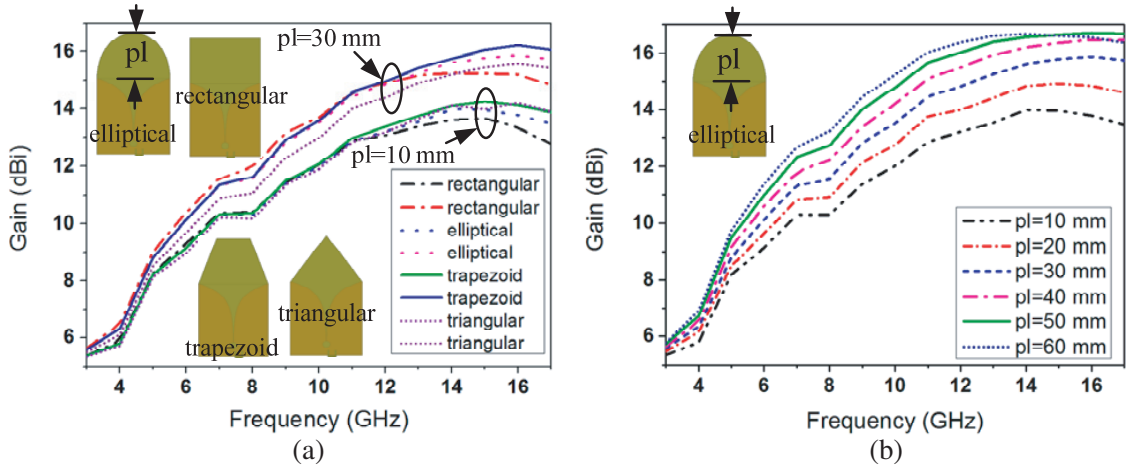

Figure 11. Gain variations of the SP-DSCVA with (a) different shaped profiles as well as (b) different lengths of the elliptical-shaped profile.

provide effective energy focusing. For easy fabrication and use, we choose the elliptical-shaped profile to construct the SP-DSCVA. Fig. 11(b) presents the result of the parametric study on the length of the elliptical-shaped profile. As can be seen, the highest value of gain is realized at $l > 50$ mm. More increase of length of the elliptical-shaped will lead to a high profile SP-DSCVA, which is not suitable for practical applications. As a result, the length of the elongated and shaped profile equals half the width of the CVA for our application and is 26 mm resulting in semicircular-shaped profile. The gains of the SP-DSCVAs with different dielectric materials are also investigated, and the results are presented in Fig. 9. It can be found that the conclusion in Section 2.2 is also applied to the SP-DSCVA. Note that more gain increase is achieved at expense of overall length. The extended length of the dielectric sheet can be seen as antenna gain regulator and depends on the gain requirement and practical space limitation.

In order to further understand the behavior of the dielectric slab, E-field distributions on the H-plane at 10 GHz and 14 GHz are illustrated in Fig. 12. It is evident that in radiation zone,the wave front of DSCVA is smoother than that of the CVA, and SP-DSCVA has the smoothest wave front resulting in higher gain than the DSCVA.

2.4. Performances of the Proposed Antennas and Discussion

Based on the above research and analysis, considering the cost-effective, the Rogers RO4003 with a thickness of 1.524 mm is used as material of the dielectric sheet to construct the proposed antenna. Fig. 2(a) illustrates the S_{11} of the proposed antennas. As can be seen, the S_{11} of these antennas are both below -10 dB from 3.5 GHz to 16.5 GHz. The loading of dielectric sheets does not destroy the impedance bandwidth of the CVA. Instead, the impedance matching in the range is improved.

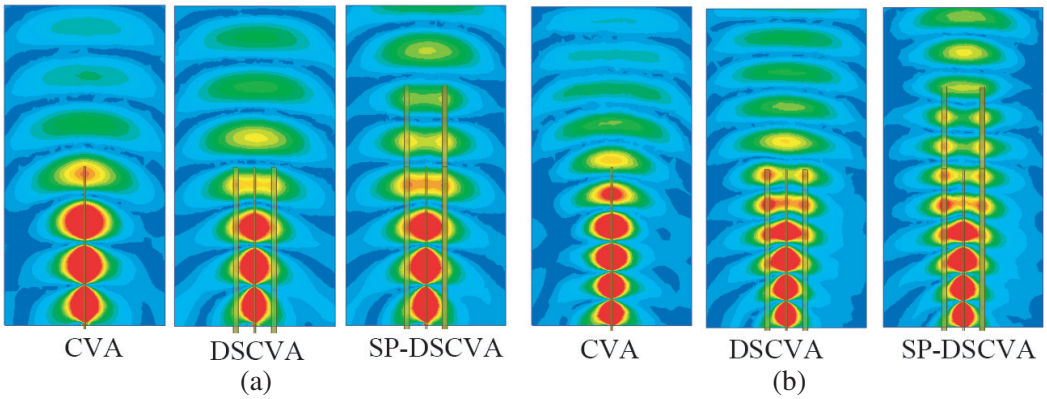

Figure 12. E-field distributions for yz-plane (H-plane) of the three antennas at 10 GHz and 14 GHz. Color bar of amplitude range is shown in Fig. 5.

Comparison of the gains for the proposed antennas is made with the result shown in Fig. 2(b). With dielectric slabs, a significant gain improvement is achieved. The gain variation of the proposed DSCVA is 5.5–13.3 dBi over 3.5 GHz–16.5 GHz, which corresponds to a gain enhancement of 0.5–5.4 dBi. Gain of the SP-DSCVA is 0.3–2.5 dBi more than that of the DSCVA in the range. Note that the higher gain performance of SP-DSCVA than the DSCVA results from the elongated tapered profile. In addition, we study the cross-polarization-level of the DSCVA and find that it is almost unaffected because the dielectric slabs are symmetrically placed.

3. EXPERIMENTAL RESULTS AND DISCUSSION

Photographs of the fabricated CVA, DSCVA and SP-DSCVA are illustrated in Fig. 13. The reflection coefficients S_{11} are measured by Agilent N5244A vector network analyzer in our laboratory. As shown in Fig. 2(a), all the antennas operate over 3.5 to 16.5 GHz. The radiation performances are tested using an NSI measurement system in an anechoic chamber. Fig. 2(b) draws the measured boresight gains of the antennas. A good agreement can be seen between simulated results and measured data. It is evident that the decreasing trend of the CVA is eliminated. The loaded dielectrics measurably enhance the gain. The increase of the gain is about 0.4–5.1 dBi for the DSCVA and 0.9–7.6 dBi for the SP-DSCVA compared to the CVA in the band. The comparison between current models with previous researches is shown in Table 2.

Figure 14 illustrates the measured radiation patterns of the CVA, DSCVA, and SP-DSCVA at 5,

Table 2. Comparison of the proposed antenna with the designs in the references.

Ref.	Size $(l \times w \times h)/\lambda_l$	Relative permittivity	O.B.W (GHz)	Gain (dBi)
[5]	$2.1 \times 1.12 \times 0.06$	2.5	6–20	9–12.09
[7]	$1.66 \times 0.5 \times 0.0315$	2.55	3–18	2–14
[13]	$1.45 \times 0.52 \times 0.005$	2.2	3–11	3.5–12.5
[19]	$1.64 \times 0.84 \times 0.02$	2.2	6–19	7.2–12
[24]	$0.93 \times 0.67 \times 0.267$	3.38	2–18	3–12.3
DSCVA	$0.74 \times 0.61 \times 0.163$	3.38	3.5–16.5	5.3–13.1
SP-DSCVA	$1.05 \times 0.61 \times 0.163$	3.38	3.5–16.5	5.72–15.3

'λ_l': the wavelength of low end frequency; 'O.B.W': operating bandwidth.

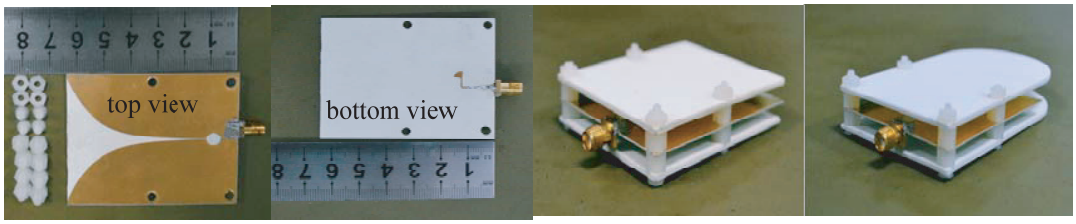

Figure 13. Fabricated antennas. (a) CVA, (b) DSCVA, and (c) SP-DSCVA.

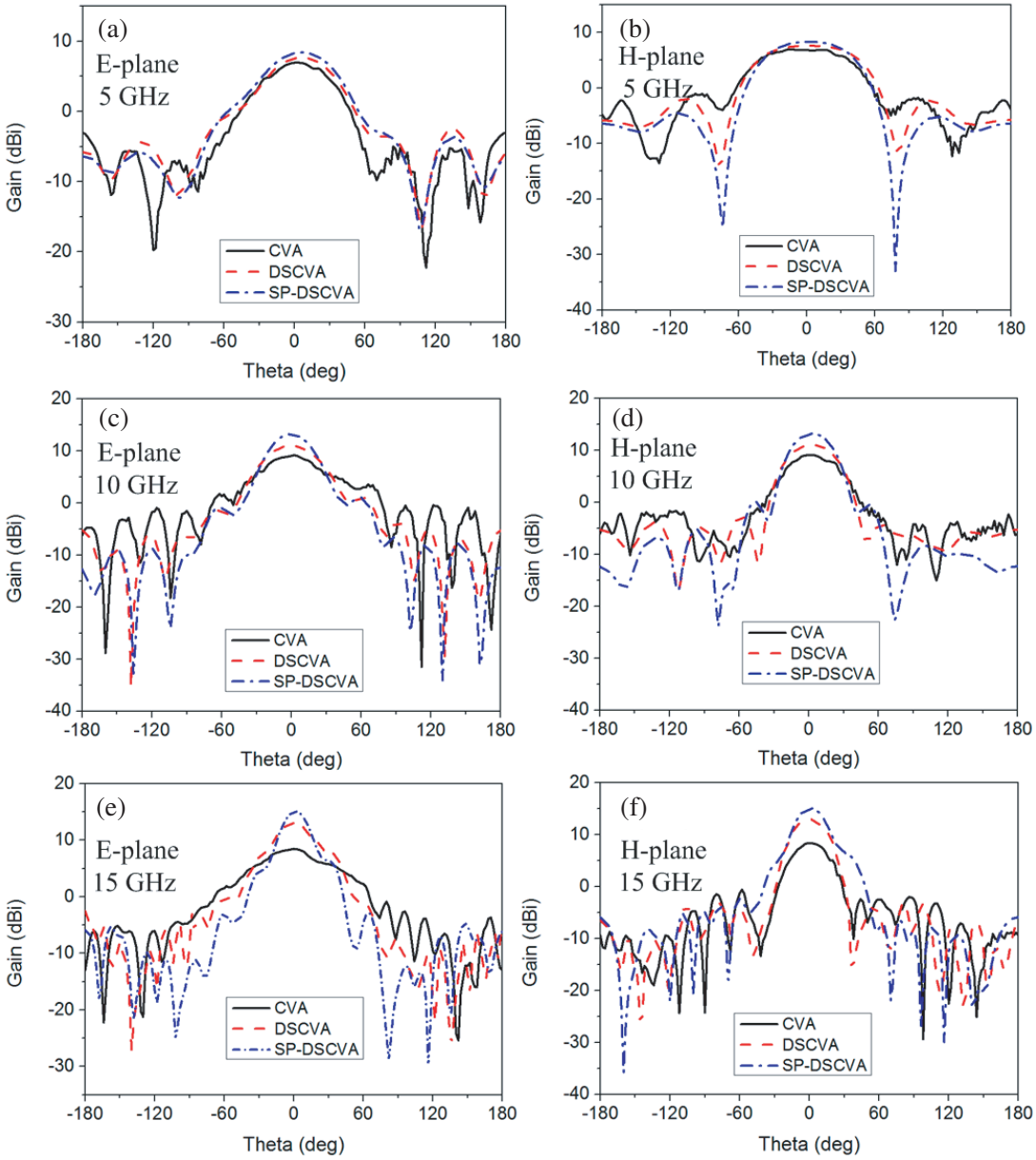

Figure 14. Measured radiation patterns of the three antennas both in the E- and H-plane at 5 GHz, 10 GHz, and 15 GHz.

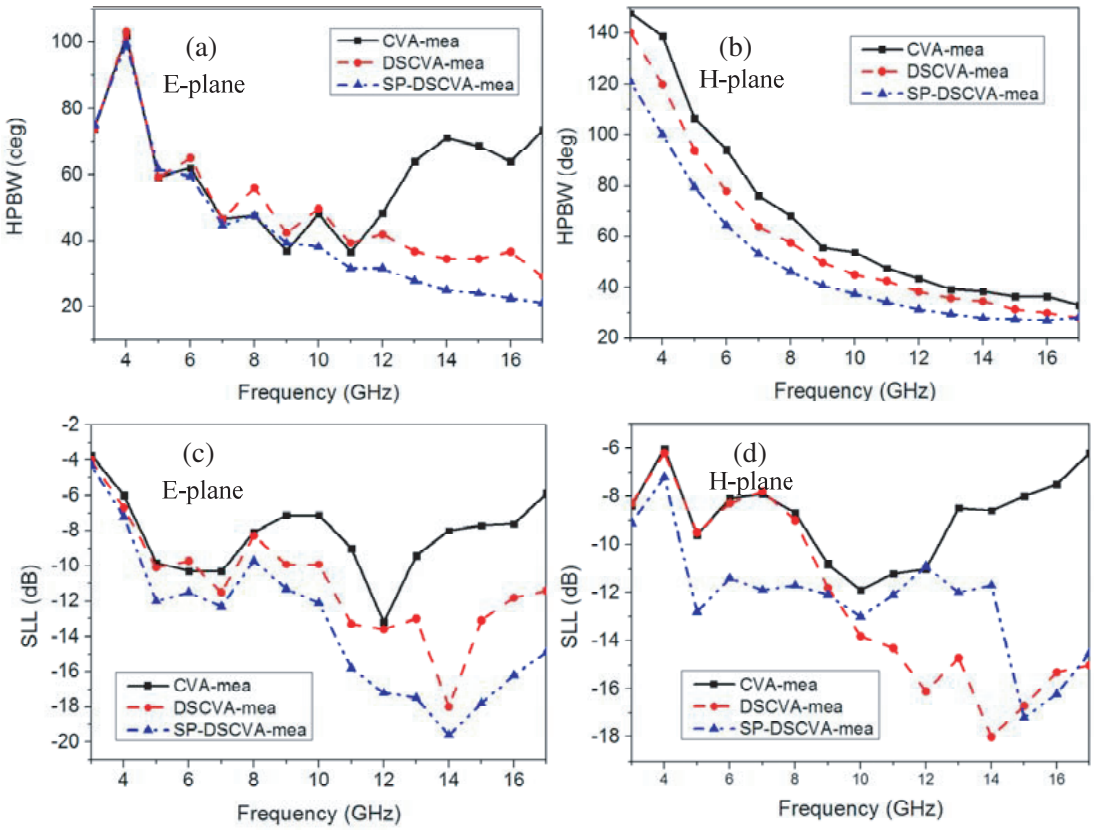

Figure 15. Measured HPBW and SLL.

10, and 15 GHz for E-plane (xz-plane) and H-plane (yz-plane). It can be observed the DSCVA and SP-DSCVA own narrower half-power beamwidth (HPBW) and smaller sidelobe level (SLL) than the CVA in both E- and H-planes at higher frequencies. The detailed frequency responses of HPBW and SLL are demonstrated in Fig. 15. The wide E-plane HPBWs resulting from the aperture phase errors at higher frequencies are obviously improved. Since the H-plane HPBW is sensitive to the length of the tapered slot, the improvement is not so remarkable as that in E-plane, and the extended length of the shaped profile makes the HPBW of the SP-DSCVA narrower than that of the DSCVA. In addition, the SLLs of the CVA are reduced in both E- and H-planes at higher frequencies by the dielectric slabs. It should be mentioned that this method has the potential of correcting the problem of tilted beam for the ultra-wideband TSA with bandwidth up to multiple-octave or one-decade at high frequencies. Due to the bandwidth limitation of the CVA, this phenomenon is not obvious here.

4. CONCLUSION

A simple technique for improving the Vivaldi antenna gain based on stacking dielectric sheets spaced by an air layer of suitable thickness with the antenna board is presented. The dielectric sheets couple with the CVA, leading to decrease of the intensisty of the surface current at the flare termination, and transform the space waves emitting from the CVA to guided waves. The guided waves can generate smooth wavefront and increase the effective antenna radiation aperture, which contribute to the increase of the gain. The CVA and proposed dielectric slabs-covered Vivaldi antennas are fabricated and measured for verification. The results show that the DSCVA provides a gain variation of 5.3–13.1 dBi with short length from 3.5 to 16.5 GHz. The extended elliptical-shaped DSCVA achieves higher gain of 5.72–15.3 dBi. The gain enhancement of the SP-DSCVA is 0.9–7.6 dBi compared to the CVA. This effective approach can be applied in the microwave imaging system.

REFERENCES

1. Gibson, P. J., "The Vivaldi aerial," *Proc. IEEE 9th Eur. Microw. Conf.*, 101–105, 1979.
2. Moosazadeh, M., S. Kharkovsky, J. T. Case, and B. Samali, "Miniaturized UWB antipodal Vivaldi antenna and its application for detection of void inside concrete specimens," *IEEE Antennas Wireless Propag. Lett.*, Vol. 16, 1317–1320, 2017.
3. Yang, Z., J. J. Huang, W. W. Wu, and N. C. Yuan, "An antipodal Vivaldi antenna with band-notched characteristics for ultra-wideband applications," *AEU — Int. J. Electron. Communs.*, Vol. 76, 152–157, 2017.
4. Mark, R., W. van Cappellen, E. van der Wal, M. Arts, R. van der Brink, and V. Klaas, "Development of a Vivaldi tile for the SKA mid frequency aperture array," *10th European Conference on Antennas and Propagation (EuCAP)*, 1–4, 2016.
5. Kota, K. and L. Shafai, "Gain and radiation pattern enhancement of balanced antipodal Vivaldi antenna," *Electron. Lett.*, Vol. 47, No. 5, 303–304, 2011.
6. Teni, G., N. Zhang, J. Qiu, and P. Zhang, "Research on a novel miniaturized antipodal Vivaldi antenna with improved radiation," *IEEE Antennas Wireless Propag. Lett.*, Vol. 12, 417–420, 2013.
7. Molaei, A., M. Kaboli, S. A. Mirtaheri, and M. S. Abrishamian, 'Dielectric lens balanced antipodal Vivaldi antenna with low cross-polarisation for ultra-wideband applications," *IET Microw., Antennas Propag.*, Vol. 8, No. 14, 1137–1142, 2014.
8. Juan, L., F. Guang, Y. Lin, and F. Demin, "A modified balanced antipodal Vivaldi antenna with improved radiation characteristics," *Microw. Opt. Technol. Lett.*, Vol. 55, No. 6, 1321–1325, 2013.
9. Akhter, Z., B. N. Abhijith, and M. J. Akhtar, "Hemisphere lens-loaded Vivaldi antenna for time domain microwave imaging of concealed objects," *Journal of Electromagnetic Waves and Applications*, Vol. 30, No. 9, 1183–1197, 2016.
10. He, S. H., W. Shan, C. Fan, Z. C. Mo, F. H. Yang, and J. H. Chen, "An improved Vivaldi antenna for vehicular wireless communication systems," *IEEE Antennas Wireless Propag. Lett.*, Vol. 13, 1505–1508, 2014.
11. Nassar, I. T. and T. M. Weller, "A novel method for improving antipodal Vivaldi antenna performance," *IEEE Trans. Antennas Propag.*, Vol. 63, No. 7, 3321–3324, 2015.
12. Fei, P., Y. C. Jiao, W. Hu, and F. S. Zhang, "A miniaturized antipodal Vivaldi antenna with improved radiation characteristics," *IEEE Antennas Wireless Propag. Lett.*, Vol. 10, 127–130, 2011.
13. In, D.-M., M.-J. Lee, D. Kim, C.-Y. Oh, and Y.-S. Kim, "Antipodal linearly tapered slot antenna using unequal half-circular defected sides for gain improvements," *Microw. Opt. Technol. Lett.*, Vol. 54, No. 8, 1963–1965, 2012.
14. De Oliveira, A. M., M. B. Perotoni, S. T. Kofuji, and J. F. Justo, "A palm tree antipodal Vivaldi antenna with exponential slot edge for improved radiation pattern," *IEEE Antennas Wireless Propag. Lett.*, Vol. 14, 1334–1337, 2015.
15. Wang, Y. W., G. M. Wang, and B. F. Zong, "Directivity improvement of Vivaldi antenna using double-slot structure," *IEEE Antennas Wireless Propag. Lett.*, Vol. 12, 1380–1383, 2013.
16. Alhawari, A. R. H., A. Ismail, M. A. Mahdi, and R. S. A. Raja Abdullah, "Antipodal Vivaldi antenna performance booster exploiting snug-in negative index metamaterial," *Progress In Electromagnetics Research C*, Vol. 27, 265–279, 2012.
17. Zhou, B., H. Li, X. Y. Zou, and T. J. Cui, "Broadband and high-gain planar Vivaldi antennas based on inhomogeneous anistropic zero-index metamaterial," *Progress In Electromagnetics Research*, Vol. 120, 235–247, 2011.
18. Sun, M., Z. N. Chen, and X. M. Qing, "Gain enhancement of 60 GHz antipodal tapered slot antenna using zero-index metamaterial," *IEEE Trans. Antenna Propag.*, Vol. 61, 1741–1746, 2013.
19. Chen, L., Z. Y. Lei, R. Yang, J. Fan, and X. W. Shi, "A broadband artificial material for gain enhancement of antipodal tapered slot antenna," *IEEE Trans. Antennas Propag.*, Vol. 63, No. 1, 395–400, 2015.

20. Gaurav, K. P. and K. M. Manoj, "Anisotropic artificial material with ENZ and high refractive index property for high gain Vivaldi antenna design," *15th Mediterranean Microwave Symposium (MMS)*, 1–4, 2015.
21. Kumar, P., Z. Akhter, A. Kr. Jha, and M. Jaleel Akhtar, "Directivity enhancement of double slot Vivaldi antenna using anisotropic zero-index metamaterials," *International Symposium on Antennas and Propagation & USNC/URSI National Radio Science Meeting*, 2333–2334, 2015.
22. Li, X. X., L. Sang, Y. Shi, G. Q. Lv, and R. Cao, "Gain improvement of planar printed broadband end-fire antenna," *Int. J. Electro.*, Vol. 104, No. 11, 1906–1919, 2017.
23. Yngvesson, K. S., T. L. Korzeniowski, Y. S. Kim, E. L. Kollberg, and J. F. Johansson, "The tapered slot antenna – A new integrated element for millimeter-wave applications," *IEEE Trans. Microw. Theory Technol.*, Vol. 37, No. 2, 365–374, 1989.
24. Saee Arezoomand, A., R. A. Sadeghzadeh, and M. Naser-Moghadasi, "Investigation and improvement of the phase-center characteristics of Vivaldi's antenna for UWB applications," *Microw. Opt. Technol. Lett.*, Vol. 58, No. 6, 1275–1281, 2016.